International Journal of Mechanical, Industrial and Aerospace Sciences
ISSN: 2517-9950
Vol:9, No:2, 2015

Advanced Model for Calculation of the Neutral Axis Shifting and the Wall Thickness Distribution in Rotary Draw Bending Processes

B. Engel, H. Hassan

***Abstract*—**Rotary draw bending is a method which is being used in tube forming. In the tube bending process, the neutral axis moves towards the inner arc and the wall thickness distribution changes for tube's cross section. Thinning takes place in the outer arc of the tube (extrados) due to the stretching of the material, whereas thickening occurs in the inner arc of the tube (intrados) due to the comparison of the material. The calculations of the wall thickness distribution, neutral axis shifting, and strain distribution have not been accurate enough, so far. The previous model (the geometrical model) describes the neutral axis shifting and wall thickness distribution. The geometrical of the tube, bending radius and bending angle are considered in the geometrical model, while the influence of the material properties of the tube forming are ignored. The advanced model is a modification of the previous model using material properties that depends on the correction factor. The correction factor is a purely empirically determined factor. The advanced model was compared with the Finite element simulation (FE simulation) using a different bending factor (B_f =bending radius/ diameter of the tube), wall thickness (W_f = diameter of the tube/ wall thickness), and material properties (strain hardening exponent). Finite element model of rotary draw bending has been performed in PAM-TUBE program (version: 2012). Results from the advanced model resemble the FE simulation and the experimental test.

***Keywords*—**Rotary draw bending, material properties, neutral axis shifting, wall thickness distribution.

I. Introduction

DUE to its high forming advantages, the NC bending process of thin-walled tubes have been attracting more and more applications in aerospace, aviation, automobile and various other high technology industries as well as it has been satisfying the increasing needs for high strength / weight ratio products. The technology has become one of the main fields in the research and development of advanced plastic forming technology [1].

During the process, the forward tangent of the tube is fixed between the inner and the outer clamp dies. It is drawn around the rotating bend die while the pressure die is used an abutment to hold the back tangent of the tube. The wiper die interactions with mandrel avoid wrinkles on the intrados of the tube [2] (see Fig. 1).

Prof. Dr.-Ing. Bernd Engel is the head the Chair of Forming Technology, Department of Mechanical Engineering, University of Siegen, 57076 Siegen, Germany.

M. Sc. Hassan Raheem Hassan is PhD student at the Chair of Forming Technology, Department of Mechanical Engineering, University of Siegen, 57076 Siegen, Germany. Master degree in University of Baghdad, Baghdad, Iraq (Corresponding author: e-mail: Hassan.Hassan@uni-siegen.de).

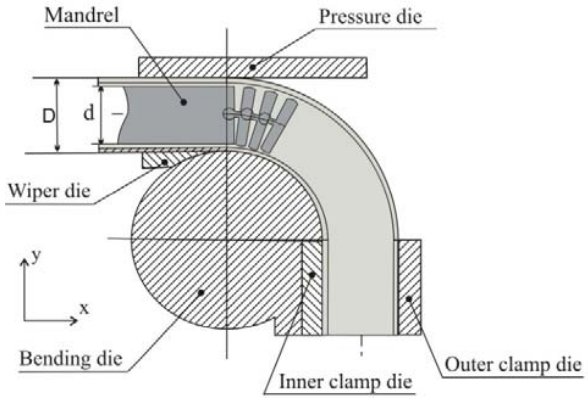

Fig. 1 Tools for the rotary draw bending processes

In This study, the geometrical model has been developed to obtain a new advanced model. The advanced model is performed with material properties to calculate the neutral axis shifting and the wall thickness distribution. The geometrical model was the previous work to calculate the neutral axis shifting and wall thickness distribution that depended on the geometrical of the tube, bending radius, and bending angle. In addition, an FE simulation of the rotary draw bending has been developed and compared with the results obtained using the advanced model.

II. Previous Model

The geometrical model has been developed to calculate the neutral axis shifting as well as a wall thickness distribution with different bending angles [3]. This model based on the calculation of [4], where the maximum amount of the neutral axis shifting is calculated from:

$$R_b^{`} = \sqrt{R_i . R_o} \quad (1)$$

$$e_i = R_b - R_b^{`} \quad (2)$$

where R_b shows the bending radius (the distance from the center of the tube to the center of the bending die), R_i is the distance from the center of the bending die to the inner arc of the tube, R_o is the distance from the center of the bending die to the outer arc of the tube, R_b' is the distance from the center of the bending die to the neutral axis after shifting and e_i is the maximum amount of the neutral axis shifting using basic model. The neutral axis shifting has different values for

different bending angles that can be obtained according to the following assumption: the neutral axis shifting is derived from (2) at a bending angle of 90°. By using half of the bending angle (45°), the following equation expresses the neutral axis shifting for different bending angles (3):

$$e_\alpha = \frac{e_i}{sin\,45} \,.\, sin\,(\frac{\alpha}{2}) \quad (3)$$

In the above equation, e_i is the maximum amount of the neutral axis shifting using the basic model (2); e_α is the distance of the neutral axis shifting using the geometrical model and α is the bending angle.

III. Advanced Model Calculation

The material properties have an influence on the neutral axis shifting, wall thickness distribution and strain distribution. The advanced geometrical model has been developed to calculate the neutral axis shifting and the wall thickness distribution. The model is modified with material properties using the correction factor. The correction factor is a purely empirically determined. The correction factor is shown by:

$$C_T = \left|\ln \frac{n.R_b}{t_o.100}\right| \quad (4)$$

where C_T is the correction factor, n is the strain hardening exponent, R_b is the bending radius and t_o is the original wall thickness of the tube. The following equations express a new neutral axis shifting in the tube and a new bending radius.

$$e_A = e_\alpha . C_T \quad (5)$$

$$R_{b.th}^{`} = R_b - e_A \quad (6)$$

where e_α is the distance of the neutral axis shifting using the geometrical model, e_A is the distance of the neutral axis shifting using the advanced model, $R_{b.th}^{`}$ is the new bending radius after neutral axis shifted using the advanced model and R_b is the bending radius.

The longitudinal strain involves two parts; one part due to the tensile strain (ϵ_t the strain at the middle of the tube) and the other part due to the bending strain (ϵ_b the strain at the upper and lower of the tube) [3]-[5] (see Fig. 2).

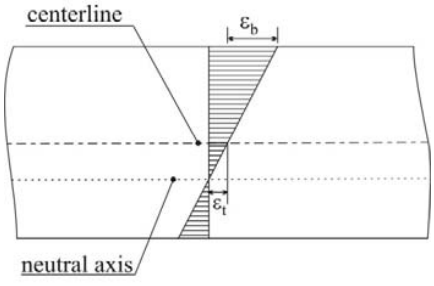

Fig. 2 Strain distribution in the rotary draw bending

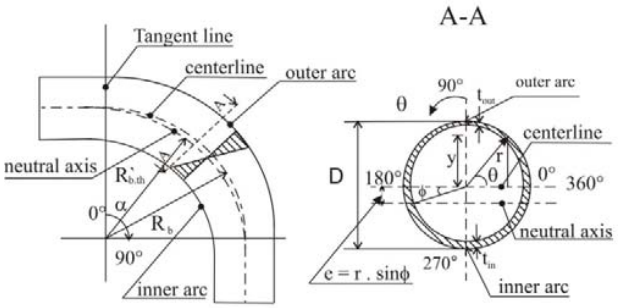

Fig. 3 Geometry of the tube and wall thickness distribution in rotary draw bending processes

Based on these calculations, the model has been developed to calculate the longitudinal strain and the wall thickness distribution with new bending radius. Fig. 3 demonstrates the geometry of the tube and a tube's cross section after bending. The original neutral axis of the tube is denoted in the center of the tube and the distance from the center of the tube to the center of the bending die is called bending radius (R_b). The neutral axis is moved toward the inner arc. The distance between the center of bending die to the neutral axis after shifted is called the bending radius after neutral axis shifted ($R_{b.th}^{`}$). The wall thickness distribution of the tube's cross section is characterised by thinning in the outer arc of the tube (t_{out}) and thickening in the inner arc of the tube (t_{in}).

$$\varphi_\alpha = \varphi_{\alpha t} + \varphi_{\alpha b} \quad (7)$$

$$\varphi_\alpha = \ln\left(\frac{L_s}{L_o}\right) + \ln\left(1 + \frac{y}{R_b}\right) \quad (8)$$

$$L_s = R_b \,.\, \alpha \quad (9)$$

$$L_o = R_{b.th}^{`} \,.\, \alpha \quad (10)$$

where φ_α is the true strain, $\varphi_{\alpha t}$ is the true tensile strain, $\varphi_{\alpha b}$ is the true bending strain, all in the longitudinal direction, L_s is the length of the fiber in the center of the tube, L_o is the original length of the tube, R_b is the bending radius, $R_{b.th}^{`}$ is the advanced bending radius after neutral axis shifting using the advanced model and α is the bending angle. y denotes the distance between any point on the tube and the center line of the tube, and is calculated from:

$$y = r \,.\, sin\theta \quad (11)$$

where θ is the angle in the cross section of the tube oriented from the neutral axis and r is the radius of the tube. Hence, y is positive in the outer arc and negative in the inner arc shown in Fig. 3.

The following calculation of the wall thickness variation is under the assumption that "the volume of the tube material is considered constant and the material is considered homogeneous". Moreover, by considering the assumption of the strains in the circumference and thickness directions, it will be equal in magnitude. The strain in the circumferential

direction shows by:

$$\varphi_\theta = \varphi_s = -\frac{1}{2}\varphi_\alpha \quad (12)$$

where φ_α is the true strain in the longitudinal direction and φ_θ is the true strain in the circumferential direction. φ_s is the true strain in the thickness direction. It could be expressed in:

$$\varphi_s = ln\frac{t_{new}}{t_o} \quad (13)$$

According to these assumptions and from substituting ((8) and (13)) in (12), the new wall thickness is expressed in (14):

$$ln\frac{t_{new}}{t_o} = -\frac{1}{2}\left(\ln\left(\frac{L_s}{L_o}\right) + \ln\left(1+\frac{y}{R_b}\right)\right) \quad (14)$$

$$t_{new} = \frac{t_o}{\sqrt{\frac{l_s\cdot\left(1+\frac{y}{R_b}\right)}{L_o}}} \quad (15)$$

The wall thickness changing is calculated from:

$$\text{wall thickness chaning (\%)} = \frac{t_{new}-t_o}{t_o}.100 \quad (16)$$

where t_o expresses the original wall thickness, t_{new} is the wall thickness after bending. Hence, the wall thickness changing (%) will be negative in the outer arc and positive in the inner arc.

IV. Comparison of the Advanced Model

The advanced model was compared with finite element simulation and experimental test. The bending tests are carried out using a CNC bending machine that was produced by the Tracto-Technik GmbH & CO.KG Company. The bending machine is equipped with special parameters for this work, see Table I.

TABLE I
DIMENSIONS OF THE TOOLS AND BENDING PARAMETERS IN EXPERIMENTAL TEST

Parameters	Values
R_b (Bending radius)	75 mm
L_c (length of the clamp die)	40 mm
L_p (Length of the pressure die)	300 mm
L_w (Length of the wiper die)	140 mm
F_p (Pressure force)	45 kN
F_c (Clamp force)	70 kN
W_f (Wall Thickness Factor)	20
B_f (Bending Factor)	1.87
D (Outer diameter of the tube)	40 mm
t_o (Original wall thickness)	2mm

The finite element model was performed in PAM-TUBE program and has been developed with the experimental test parameters and other parameters (see Fig. 4).

The mechanical properties of the tube are obtained from the uniaxial tensile test. The characteristic material values are yield strength $R_{p0,2}$, tensile strength R_m, uniform elongation A_g and strain hardening exponent, which are all determined to define the material model for the finite element model, see Table II.

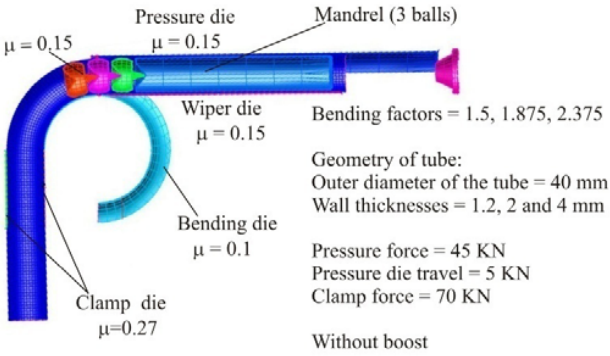

Fig. 4 Finite element model of the rotary draw bending processes

TABLE II
MATERIAL PROPERTIES

Material	Yield stress	Tensile strength	Uniform elongation	Strain hardening exponent
1.4301	464.01 N/mm²	706.95 N/mm²	44.68	0.3694
1.0036	302.87 N/mm²	417.32 N/mm²	21.28	0.1929

A. Wall Thickness Distribution and Wall Thickness Factor

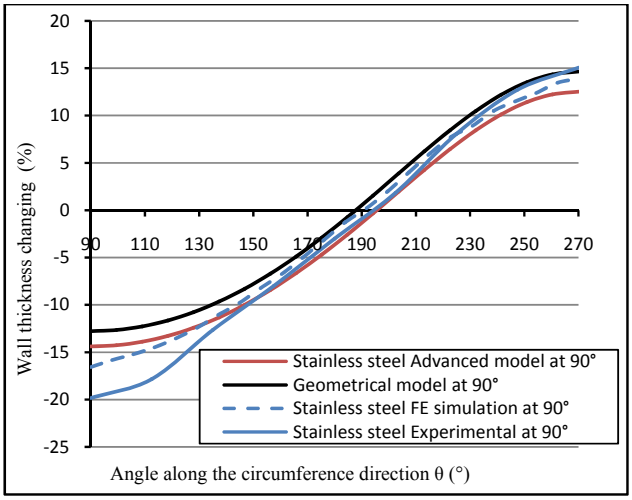

Fig. 5 Comparison of the wall thickness distribution in the cross section of the tube obtained using the advanced model , the FE simulation, the experimental test (in the middle of the bend, bending angle of 90°), for stainless steel alloy

The wall thickness distribution is influenced by the material properties. As shown in Figs. 5 and 6, that the wall thickness is thinner in the extrados and thicker in the intrados due to tension and compression, respectively. The distribution of the wall thickness in the tube's cross section was in the middle of the bend at a bending angle of 90°. The results using the advanced model are closer to the experimental test and the FE-simulation results than the results using the geometrical model. Fig. 5 shows the results of the wall thickness

distribution with a stainless steel tube obtained using the experimental test, the finite element simulation and the advanced model. Fig. 6 demonstrates the results of the wall thickness distribution with a steel tube obtained using the experimental test, the finite element simulation and the advanced model.

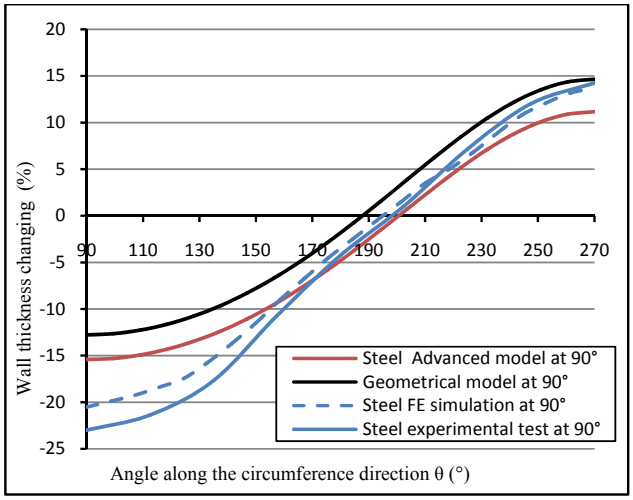

Fig. 6 Comparison of the wall thickness distribution in the cross section of the tube obtained using the advanced model , the FE simulation, the experimental test (in the middle of the bend, bending angle of 90°), for Steel alloy

In order to validate the advanced model with the different wall factors (wall factor = tube diameter / wall thickness), the wall factors were set to 33.33, 20 and 10. The diameter of the tube was 40 mm, the bending radius was 75 mm and all results were at a bending angle 90°. Fig. 7 shows the neutral axis shifting with the different wall factors. The advanced model has a good result with FE simulation than the results using the geometrical model. In comparison, the geometrical model has constant values with different wall factors.

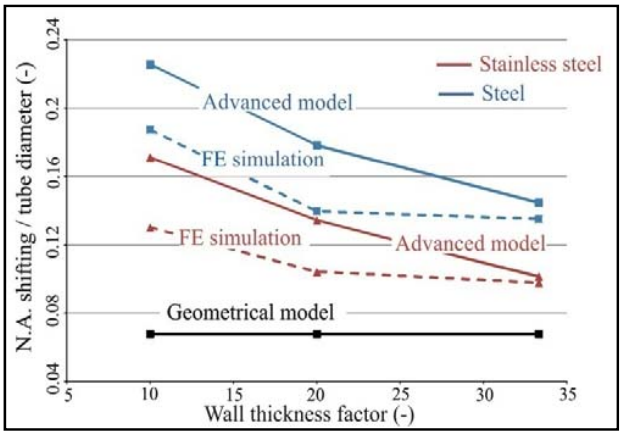

Fig. 7 Neutral axis shifting with the different wall thickness factors calculated using the advanced model, the FE simulation and the geometrical model

B. Bending Factor

To validate the advanced model with the different bending factors (bending factor = bending radius / tube diameter), the wall factor and the diameter of the tube were fixed in this comparison. The bending factors were 1.5, 1.875 and 2.375. Figs. 8 and 9 show the neutral axis shifting with the different bending factors. The results using the advanced model are closer to the FE simulation results than the results using the geometrical model.

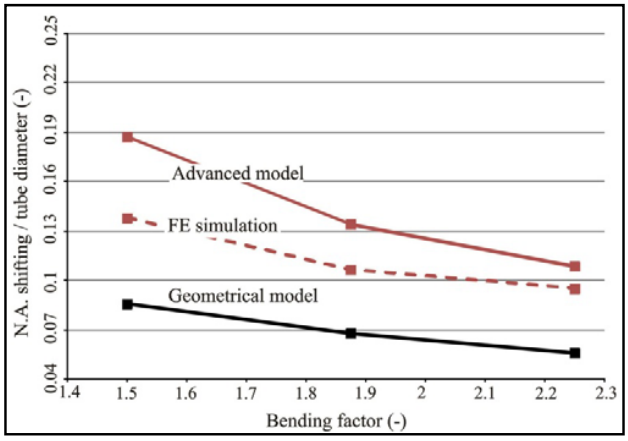

Fig. 8 Neutral axis shifting with the different bending factors calculated using the advanced model, the FE simulation and the geometrical model for Stainless steel alloy

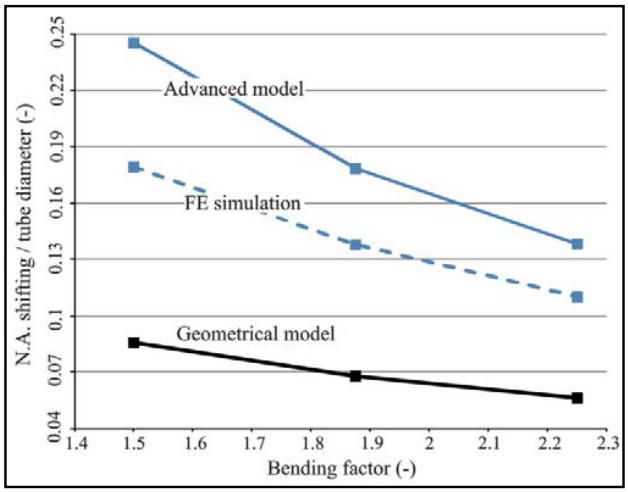

Fig. 9 Neutral axis shifting with the different bending factors calculated using the advanced model, the FE simulation and the geometrical model for steel alloy

C. Material Properties

The material properties have a great influence on the resulting neutral axis shifting. Fig. 10 shows the neutral axis shifting with the different material properties (strain hardening exponent) but the same other parameters. By using the advanced model and the FE simulation, it could be found out that the neutral axis shifting is higher for small strain hardening exponent than for high strain hardening exponent.

In comparison, the geometrical model has constant values with different material properties.

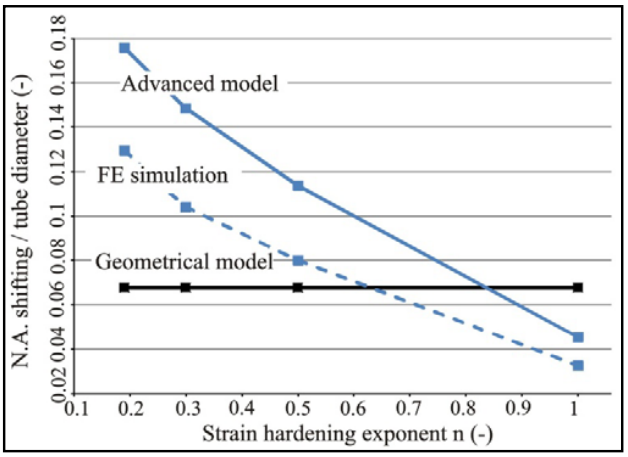

Fig. 10 Influence of the strain hardening exponent on the neutral axis shifting obtained using the advanced model, the FE simulation and the geometrical model

V. Conclusion

In this work we showed that the material properties have an influence on the neutral axis shifting. The neutral axis of the tube moves more towards the inner arc of the tube in steel alloy than in stainless steel tubes. Furthermore, we also saw that the material properties have an influence on the wall thickness distribution. The advanced model for calculating the neutral axis shifting and the wall thickness distribution has been developed. The new model considers the influence of the material properties in the bending processes. The material properties in the model are presented using strain hardening exponent. The model based on empirically determined factor. Therefore, a more accurate of the wall thickness distribution and neutral axis shifting calculations in this theoretical account is possible. The results using the advanced model are closer to the FE simulation results than the results using the geometrical model. The geometrical model has constant values with the different wall factors. The advanced model was compared with the FE simulation and experimental tests.

Another research field is to determine the influence of the material properties with thicker wall thickness. The aim is to get bends with smaller wall thickness factor.

Acknowledgment

The author would like to thank the DAAD (Deutscher Akademischer Austausch Dienst) and the Ministry of Higher Education and Scientific Research of Iraq for their contribution to this study.

References

[1] H. Yang, Z.C. Sun, Y. Lin, M.Q. Li, Advanced plastic processing technology and research progress on tube forming, Journal of Plasticity Engineering 8 (2) (2001) 86–88.
[2] B. Engle, M. Hinkel, S. Kersten, C. Mathes: VDI 3430 – Rotray Draw Bending of Profiles, Beuth Verlag, (2011).
[3] B. Engel, H. Hassan: Investigation of Neutral Axis Shifting in Rotary Draw Bending Processes for Tubes. Steel research int. (2014).
[4] Duncan J. L., Hu J., and Marciniak Z., Mechanics of Sheet Metal Forming, Butterworth-Heinemann, Woburn, MA.
[5] J. Wang, and R. Agarwal: Tube bending under axial force and internal pressure, ASME, Vol. 128,May 2006.